A mouse model of myosin binding protein C human familial hypertrophic cardiomyopathy.

Q Yang, … , R Klevitsky, J Robbins

Research Article

Familial hypertrophic cardiomyopathy can be caused by mutations in genes encoding sarcomeric proteins, including the cardiac isoform of myosin binding protein C (MyBP-C), and multiple mutations which cause truncated forms of the protein to be made are linked to the disease. We have created transgenic mice in which varying amounts of a mutated MyBP-C, lacking the myosin and titin binding domains, are expressed in the heart. The transgenically encoded, truncated protein is stable but is not incorporated efficiently into the sarcomere. The transgenic muscle fibers showed a leftward shift in the pCa2+-force curve and, importantly, their power output was reduced. Additionally, expression of the mutant protein leads to decreased levels of endogenous MyBP-C, resulting in a striking pattern of sarcomere disorganization and dysgenesis.

Find the latest version:

https://jci.me/3880/pdf

A Mouse Model of Myosin Binding Protein C Human Familial Hypertrophic Cardiomyopathy

Qinglin Yang,* Atsushi Sanbe,* Hanna Osinska,* Timothy E. Hewett,* Raisa Klevitsky,* and Jeffrey Robbins*

*Department of Pediatrics, Division of Molecular Cardiovascular Biology, Children's Hospital Research Foundation, Cincinnati, Ohio 45229-3039

Abstract

Familial hypertrophic cardiomyopathy can be caused by mutations in genes encoding sarcomeric proteins, including the cardiac isoform of myosin binding protein C (MyBP-C), and multiple mutations which cause truncated forms of the protein to be made are linked to the disease. We have created transgenic mice in which varying amounts of a mutated MyBP-C, lacking the myosin and titin binding domains, are expressed in the heart. The transgenically encoded, truncated protein is stable but is not incorporated efficiently into the sarcomere. The transgenic muscle fibers showed a leftward shift in the pCa^{2+}–force curve and, importantly, their power output was reduced. Additionally, expression of the mutant protein leads to decreased levels of endogenous MyBP-C, resulting in a striking pattern of sarcomere disorganization and dysgenesis. (*J. Clin. Invest.* 1998. 102:1292–1300.) Key words: hypertrophy • mouse • transgenic • cardiomyopathy • heart

Introduction

Familial hypertrophic cardiomyopathy (FHC)[1] is an inherited cardiac disease with a prevalence of 0.2% in the general population (1). FHC is transmitted as an autosomal dominant trait and is the leading cause of sudden death in the young, overtly healthy population. Early on, it was recognized that FHC mapped to multiple loci. Soon after the first reports linking the disease to β-*MyHC*, gene linkage/positional cloning approaches defined additional disease loci and identified mutations in other sarcomeric protein genes: chromosome 1q31 (cardiac troponin T), 15q2 (α-tropomyosin), 3p (ventricular isoform of the regulatory myosin light chain), 11p13-q13 (cardiac myosin binding protein C [MyBP-C]), 12q2 (ventricular isoform of the cardiac essential myosin light chain), and 19p13.2-q13.2 (cardiac troponin I) (2–7). Another disease locus on chromosome 7, linked to FHC with Wolff-Parkinson-White syndrome, has also been identified (8), but the gene has not yet been determined. In common, these mutations result in a "disease of the sarcomere" (6) although morbidity and mortality outcomes are highly variable and depend upon the particular mutation.

With respect to the above-mentioned genes, the cardiac isoform of MyBP-C is least well understood in terms of its basic function(s) and therefore, the pathogenic processes resulting from the genetic lesion(s) remain obscure. The contractile apparatus of muscle is a precisely assembled unit with three major filaments consisting of titin and the thick and thin filaments. The titin filament is responsible for the elasticity of relaxed striated muscle, and also acts as a molecular scaffold for thick filament formation (9). The thick filament contains the motor proteins and interacts with the actin thin filament to generate force. The role of MyBP-C, a myosin and titin binding protein located in the inner third of the A-band of striated muscle (10), is obscure. MyBP-C is relatively large ($\sim 130{,}000$ M_r) and represents ~ 2–4% of total myofibrillar protein (10). It is represented in the genome as a family, with slow skeletal, fast skeletal, and cardiac-specific isoforms and probably has both structural and signaling roles in the heart. Its structural function(s) in striated muscle have not been demonstrated directly, and the few data that exist are restricted to the skeletal isoforms. However, it may be involved in either assembly or maintenance of the thick filament, since it has both myosin and titin binding domains (11). As noted above, it is restricted to the A-band of the sarcomere, and forms a series of seven to nine transverse bands or stripes that are spaced at 43-nm intervals. The protein belongs to the immunoglobulin superfamily and its three isoforms show a highly conserved structure consisting of IgI and fibronectin domains (12). A large number (currently > 19) of mutations in cardiac MyBP-C has been linked to FHC, with most resulting in reading frame shifts and premature termination as a result of the generation of a nonsense codon (3, 13–16). The truncations most frequently include the titin and/or the myosin binding regions that are located in the COOH-terminal one-third of the molecule. The COOH-terminal 102 amino acids in the last repeated domain of MyBP-C are essential for myosin binding (17, 18). Through interactions with titin, MyBP-C can influence passive tension, a factor that can help determine the shortening velocity of cardiac fibers (19).

1. *Abbreviations used in this paper:* FHC, familial hypertrophic cardiomyopathy; MyBP-C, myosin binding protein C; MyHC, myosin heavy chain; NTG, nontransgenic; TG, transgenic.

To date, FHC-linked mutations that have been studied in some detail show a strong dominant-negative effect. That is, they are missense mutations which cause cardiac malfunction by producing a "poison polypeptide" (for review see reference 20). However, the MyBP-C–linked class of FHCs present as relatively benign phenotypes. When endomyocardial biopsies derived from an MyBP-C FHC patient were studied, no mutated MyBP-C protein was detected (21) and so it is unclear if the truncated MyBP-C protein is stable. While a single case–based report obviously does not rigorously exclude a poison polypeptide causing MyBP-C FHC, the data are partially consistent with a null allele mechanism that could cause functional haploinsufficiency by resulting in a reduced amount of the functional protein due to the instability of the truncated species.

Despite the well-established genetic etiology, the pathogenic processes leading to FHC are unclear. Longitudinal pathological changes linked to the disease state in the MyBP-C patients are hard to obtain because of the nature of the disease: the overall phenotype is benign with very mild hypertrophy presenting at mid-life, and ethical considerations preclude invasive procedures. Indeed, for the MyBP-C patient population, no published pathology exists, as the diagnoses are made by noninvasive clinical examinations using echocardiographic procedures.

In an attempt to mimic a class of MyBP-C FHC mutations we created a mouse that expresses, in the heart, a murine cardiac isoform of MyBP-C lacking both the titin and myosin binding protein sequences. Using transgenesis, multiple lines expressing different levels of the transgene were generated in order to establish a dose–response curve relating the degree of transgenic (TG) overexpression with any resulting pathology. TG mice overexpressing the normal isoform were also generated in order to ensure that a simple disruption of the normal MyBP-C stoichiometry did not occur in the cardiomyocytes as a result of changes in gene dosage. The data show that TG expression of normal MyBP-C protein is completely benign: the cardiomyocyte is able to effectively regulate the overall stoichiometry of the MyBP-C pool. However, expression of the mutated protein results in the development of a significant pathology detectable at the gross and ultrastructural levels. Although organ function is unaltered in young adults, there are significant alterations at the cardiomyocyte level with disarray and sarcomere dysgenesis presenting in both the atrial and ventricular compartments. Using skinned muscle fibers, we noted increased Ca^{2+} sensitivity to force development as well as decreased maximum power output.

Methods

DNA constructs and TG mice. A cDNA encoding the murine cardiac MyBP-C was generated using RT-PCR with primers based on the published sequence (22). Subsequent sequencing of multiple clones showed an almost exact match with the reported murine cardiac MyBP-C cDNA sequence, except for amino acids 844–866. Repeated sequencing showed consistent results and the clone's sequence matched exactly with the human sequence (GenBank accession number 1085290). Examining the published murine cardiac MyBP-C sequence, it appears that the discrepancy was due to a nucleotide skip in the previously published sequence at the beginning of the region with a shift back into frame after 23 amino acids. The cDNA (GenBank accession number AF059576) consists of 4224 bp: translation begins at 109 (some 5′ untranslated sequence was included), ends at 3921 (the clone also includes some 3′-UTR), and is flanked by unique

SalI sites. The sequence encoding the myc epitope was incorporated into the primer such that the tag was placed after the initiator methionine residue. The PCR product was sequenced and the fragment was linked to the mouse α-myosin heavy chain (α-MyHC) promoter (see Fig. 1). The final construct was digested free of vector sequence with NotI, purified from agarose gels, and used to generate TG mice as previously described (23).

RNA transcript analyses. Total RNA was prepared from freshly isolated tissues. Samples were homogenized in Tri-Reagent (Molecular Research Center, Cincinnati, OH) and total RNA was extracted according to the manufacturer's instructions. 5 μg of total RNA was loaded onto a nitrocellulose membrane (Zeta-probe; Bio-Rad, Hercules, CA) using a dot blotting apparatus (Bio-Rad). Hybridization using ^{32}P-end-labeled oligonucleotides was performed as described previously (23). In each case, the specificity of the oligonucleotide was confirmed by hybridizations to genomic Southern blots and/or Northern blots of cardiac total RNA.

Total and myofilament protein isolation, SDS-PAGE gel electrophoresis, and Western analyses. For SDS-PAGE electrophoresis, the left ventricular apex and atrial flaps were obtained from TG mice and nontransgenic (NTG) littermates that had been killed. Samples enriched for the myofibrillar proteins were isolated as described previously (24). Gel preparations, electrophoretic conditions, and gel staining have been described elsewhere (25). Western analyses were performed using anti–MyBP-C (FC-18, a generous gift from Dr. Obinata of Chiba University, Chiba, Japan) and anti–C-Myc monoclonal antibodies (Boehringer Mannheim, Mannheim, Germany).

Immunofluorescent analysis and confocal microscopy. For immunofluorescent detection of MyBP-C and/or correlated TG proteins, mice were anesthetized with isoflurane, and the hearts were perfused with relaxing buffer and fixed with 4% paraformaldehyde in PBS at 4°C. After fixation, the hearts were sucrose infiltrated in a solution containing 30% sucrose in PBS overnight at 4°C and were subsequently embedded in O.C.T. compound (Miles, Elkhart, IN). 5-μm-sections were incubated with mouse monoclonal antisera against human C-Myc epitope, and with polyclonal antibodies against desmin (Biomeda, Foster City, CA) or α-actinin (Sigma Chemical Co., St. Louis, MO). FC-18, an anticardiac MyBP-C monoclonal antibody, was also used to stain the endogenous cardiac MyBP-C to ensure the correct location of the TG proteins. Secondary antibodies used were conjugated either to FITC or to Texas red. The sections were visualized using confocal microscopy (Molecular Dynamics, Sunnyvale, CA).

Histopathological and ultrastructural analysis. For light microscopy, the heart was excised from the anesthetized mouse after injecting relaxation buffer (5% dextrose, 30 mM KCl in PBS). Hearts were fixed in 10% formalin before sectioning. Step serial longitudinal 5-μm sections of the heart was taken at every 200 μm. The sections were dehydrated through a gradient of alcohol and were paraffin embedded. The section was then stained with Gomori's trichrome. Preparation of samples for transmission electron microscopy has been described (25). Thin sections were counterstained with uranyl acetate and lead citrate and examined at Zeiss Omega 912 transmission electron microscope at accelerating voltage 100 kV.

Skinned fiber mechanical analyses. Procedures for mechanical analysis of murine "skinned" papillary fibers have been described previously (25). In brief, hearts were removed and muscle fibers (150–200 μm in diameter and 1.3–2.0 mm in length) were prepared from left ventricular papillary muscles. The fiber strips were skinned and stored at −20°C until used. All skinned fiber experiments were performed using a commercially available apparatus (Scientific Instruments, Heidelberg, Germany). Strip tension (mN/mm^2) was calculated by dividing force by fiber cross-sectional area, calculated from widths measured at the major axis. Free Ca^{2+} concentration was obtained by mixing relaxation and contraction solutions in the appropriate proportions. Unloaded shortening velocity was obtained by the slack test (26, 27). The force–velocity relationship was determined by isotonic quick releases under constant load at pCa 5.0. Load clamping for isotonic shortening was achieved by changing the mode of opera-

tion from length control to force control during isotonic steady-state force. Within 20 ms, the velocity of shortening was stable. Force values were measured by averaging the records from 9 ms to 17 ms after each step to an isotonic load. The shortening velocity and force during isotonic contraction was analyzed using a commercially available program (Scientific Instruments). The program fits a hyperbola into the measured points and extrapolates to maximum shortening velocity. The hyperbola fitted to the data is: $(F + a)(v + b) = b(F0 + a)$, where F is the force during isotonic shortening, $F0$ is isometric force, v is the isotonic shortening velocity, and a and b are characteristic constants. From the curve fit to the isotonic shortening, relative power (W) was calculated for each fiber ($W = v \cdot F/F0$).

Results

Two MyBP-C transgenes, encoding either the mouse cardiac wild-type (MyBP-C.wt) or truncated (MyBP-C.mut1) proteins, were linked to the cardiac-specific α-MyHC promoter and used to generate multiple lines of TG mice (Fig. 1 A). A C-Myc epitope sequence after the initiator methionine residue was placed into each cDNA. MyBP-C.mut1 encodes a truncated protein, which lacks both the myosin and titin protein binding domains whereas the MyBP-C.wt encodes a full-length wild-type cardiac MyBP-C protein. Three MyBP-C.wt and five MyBP-C.mut1 TG lines, expressing different levels of the transgenes, were selected for subsequent study and the degree of overexpression, relative to the endogenous MyBP-C transcripts, was established (Fig. 1 B). As expected based on other TG lines generated with this promoter construct (28, 29),

expression levels differed among different lines, varying from two- to eightfold.

TG protein expression against the endogenous MyBP-C protein background. Western blot analyses of total protein extracts prepared from the TG lines (8–12 wk) were carried out using either the anti–C-Myc or anti–MyBP-C (FC-18) monoclonal antibodies, which detect the transgenically encoded or endogenous proteins, respectively. Preliminary experiments with a number of transgenic constructs have shown that 1–2 mo is the earliest age at which the maximal amount of TG protein is present in the hearts (Robbins, J., unpublished data). The anti–C-Myc antibody detected the full-length and truncated proteins in the respective TG mouse lines (2/1 and 32, respectively) but not in the NTG littermates (Fig. 2 A). The data confirm the correct size of the transgenically encoded polypeptides and show that the truncated MyBP-C protein is stable. The truncated form was not detected by the FC-18 antibody whose epitope apparently lies in the terminal third of the molecule which was deleted in the construct.

TG protein levels and the degree of replacement or augmentation of the endogenous MyBP-C protein pool were examined further using SDS-PAGE electrophoresis. Total protein from 8–12-wk ventricles of the three highest expressing MyBP-C.mut1 lines and the three MyBP-C.wt lines, as well as their NTG littermates, was separated on 8.5% SDS-polyacrylamide gels and stained with colloidal brilliant blue (Fig. 2 B). Despite the increase in transcript levels, no concomitant increase in the levels of MyBP-C was observed in any of the three TG lines overexpressing the wild-type construct (Fig. 2
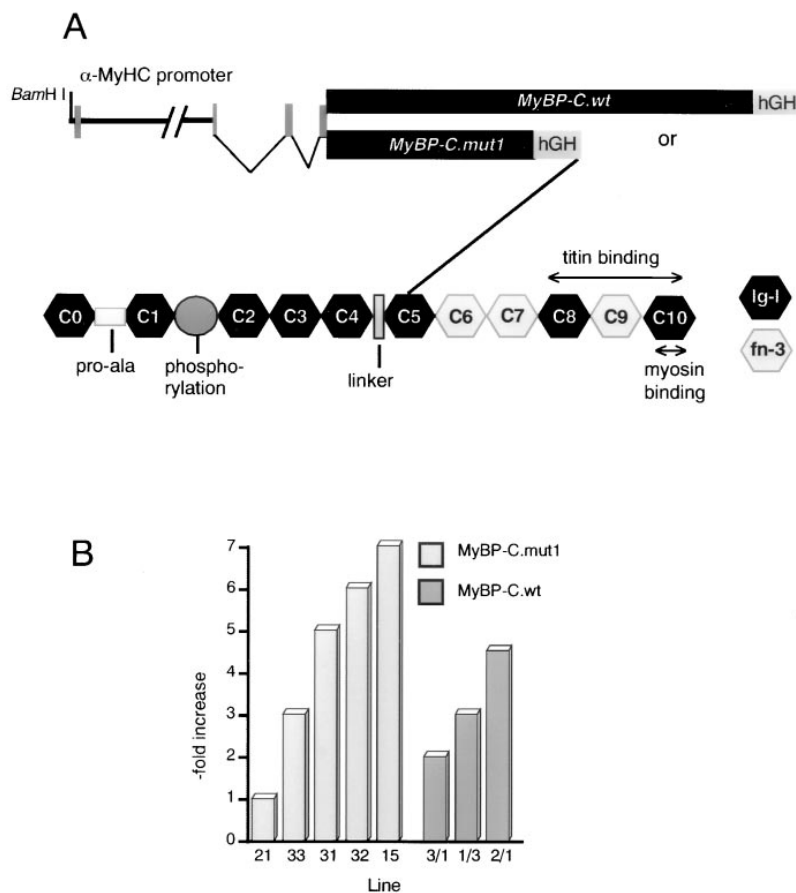

Figure 1. TG constructs and transcript expression. (*A*) Two MyBP-C transgenes, encoding either the mouse cardiac wild-type (*MyBP-C.wt*) or truncated (*MyBP-C.mut1*) proteins, were linked to the cardiac-specific α-MyHC promoter (29) and used to generate multiple lines of TG mice. As shown, MyBP-C.mut1 encodes a truncated protein which lacks both the myosin and titin protein binding sites. Both constructs contained a C-Myc epitope sequence after the initiator methionine residue. The human growth hormone polyadenylation site was placed downstream of the cDNA's. (*B*) Analyses of TG RNA expression in three MyBP-C.wt and five MyBP-C.mut1 lines. For each measurement 5 μg of total RNA isolated from ventricular tissue was loaded onto nitrocellulose and hybridized to ^{32}P-end-labeled oligonucleotides which recognize both TG and endogenous MyBP-C transcripts. Shown are the TG RNA expression levels in different lines of TG mice relative to their NTG littermates. All hybridization signals were normalized using a GAPDH signal to correct for loading variation.
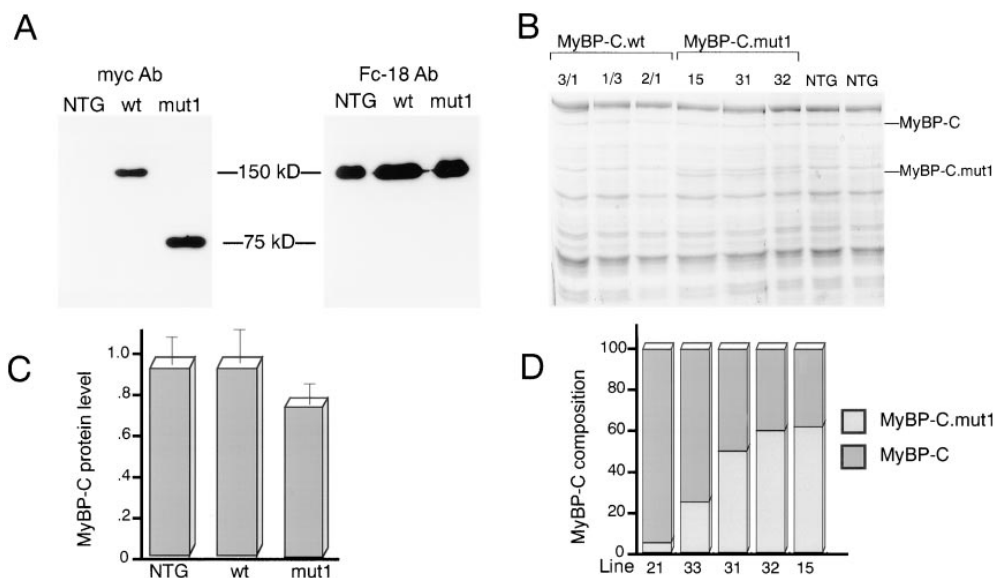
Figure 2. TG protein levels and TG protein replacement of endogenous MyBP-C. Total protein was isolated with high-salt protein extraction buffer and 10 μg was electrophoresed on 8.5% PAGE gels. (*A*) Western blot analyses using anti-Myc and anti–MyBP-C (FC-18) monoclonal antibodies detect the transgenically encoded and endogenous proteins, respectively. Material derived from 8–10-wk MyBP-C.wt (line *2/1*) or MyBP-C.mut1 (line *32*) hearts are shown. The C-Myc antibody detects the full-length and truncated proteins in the respective TG mouse lines, but not in the NTG littermates. The right panel shows the MyBP-C species detected by the FC-18 MyBP-C antibody. Only a single species was detected in the line 2/1 MyBP-C.wt–derived protein (*wt*), confirming the correct size and stability of the transgenically encoded polypeptide. The truncated line 32 MyBP-C.mut1 (*mut1*) was not detected by FC-18 as its epitope lies in the terminal third of the molecule. (*B*) Analysis of sarcomere protein composition of 8–12-wk ventricular tissue of TG lines. This time point was chosen in order to ensure that the TG protein level had reached a steady state. A representative total ventricular protein gel of the three MyBP-C.mut1 high-expressers, the three MyBP-C.wt lines, and the two NTG littermates. The endogenous MyBP-C (or MyBP-C.wt) and MyBP-C.mut1 bands are indicated. MyBP-C.mut1 protein is clearly visible whereas no detectable increase in the full-length MyBP-C protein in the MyBP-C.wt was detected. (*C*) Changes in the amount of full-length MyBP-C protein levels. Samples from MyBP-C.wt, MyBP-C.mut1, and NTG littermates were electrophoresed on SDS-PAGE, the protein gels stained with colloidal brilliant blue, scanned, and the peaks were quantitated using NIH Image software (v. 1.57). Again, 8–10-wk MyBP-C.wt (line 2/1) or MyBP-C.mut1 (line 32) hearts were used. To correct for loading variations, all peaks were normalized to either a non-myofilament protein or the actin in each lane (37). The levels of the 150-kD MyBP-C in the TG and NTG mice were determined relative to these. No difference were detected between the MyBP-C.wt mice and their NTG littermates (*n* = 6). However, a 23% decrease in the endogenous MyBP-C protein levels in the MyBP-C.mut1 mice occurred (*n* = 6, *P* < 0.05), presumably due to partial replacement of the full-length MyBP-C with the mutated species. (*D*) TG protein as a percentage of total MyBP-C protein. The relative amounts of MyBP-C and MyBP-C.mut1 proteins (normalized to their molecular masses) were determined by densitometry of the SDS gels.

B). We have noted this discordance between transcript and protein pools before in experiments in which the cardiac sarcomeric proteins are replaced with transgenically encoded peptides (23, 25, 29). Apparently, the cardiomyocyte has the capability of regulating the overall stoichiometry of at least a subset of the contractile proteins. The truncated MyBP-C species is easily detectable. Quantitative analyses were carried out on a series of similar gels and the proteins were quantitated by densitometry. While expression of the wild-type protein has no detectable effect on overall MyBP-C levels, the expression of the mutant protein leads to decreased sarcomeric levels of endogenous MyBP-C (Fig. 2 *C*). In the TG lines carrying the truncated MyBP-C protein, the percentage of the TG MyBP-C.mut1 protein relative to the total MyBP-C protein correlated roughly to their TG transcript levels. The highest percentage (achieved in line 15) was ∼ 60% (Fig. 2 *D*).

Both wild-type and mutant MyBP-C are incorporated into the sarcomere. The location of the TG proteins within the cardiomyocyte was determined. In particular, it was of interest to know if the truncated protein was capable of participating in sarcomere formation. This was determined via immunofluorescent staining using anti–C-Myc antibody against the C-Myc epitope. Heart sections (5 μm) were stained with selected antibodies before viewing under confocal microscopy. Sections from 16-wk NTG (Fig. 3 *A*) or MyBP-C.wt (line 2/1) mice (Fig. 3 *C*) labeled with either anti–MyBP-C (FC-18) or anti–C-Myc antibodies, respectively, were uniformly stained and the striation patterns were identical, indicating efficient and correct incorporation of the wild-type TG protein into the sarcomeres. The anti–C-Myc did not react with the NTG control (Fig. 2 *B*). In contrast to the normal pattern observed in the MyBP-C.wt section, anti–C-Myc staining of the MyBP-C.mut1 heart sections derived from 14-wk line 32 animals showed a patchy striation pattern and diffuse staining (Fig. 3 *E*, *left*). The same MyBP-C.mut1 section stained with α-actinin confirmed that the overall striation pattern was still conserved (Fig. 3 *E*, *right*). When sections were double-labeled with anti–C-Myc and antidesmin (which marks the Z-band), the MyBP-C.wt sarcomeres revealed a typical well-organized pattern of striation and discrete spatial locations of the two proteins (Fig. 3 *D*). In contrast, when a severely affected MyBP-C.mut1 cell was similarly stained, anti–C-Myc staining appeared as discrete striated foci but also as weaker, diffused staining in other areas (Fig. 3 *F*). The normal pattern of desmin staining was also disrupted, indicating significant sarcomere dysgenesis in this section. We conclude that the wild-type TG protein is incorporated into the sarcomere in a manner that is indistinguishable from the endogenous protein. The mutated protein, lacking the titin and myosin binding domains, is also incorporated into sarcomeres. However, incorporation did not result
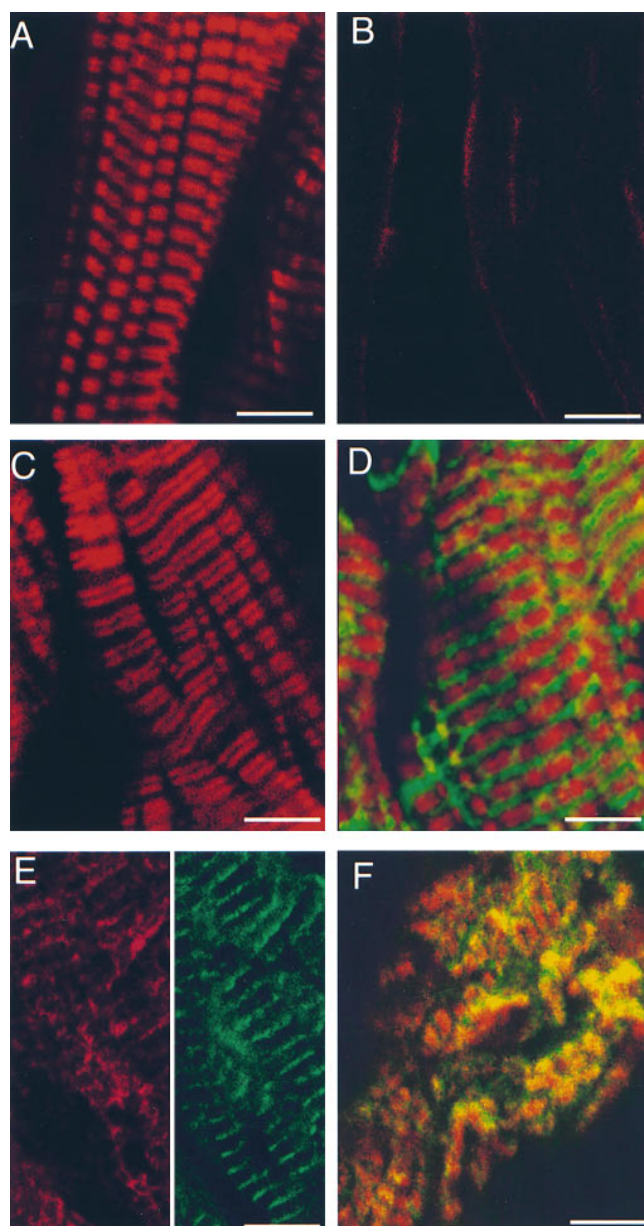
Figure 3. Immunofluorescent staining and confocal microscopy. Young adult animals, all of who appeared overtly healthy after at least 8 wk of observation upon achieving maturity, were selected for this study. Hearts from both TG and NTG mice were perfused with relaxing buffer, fixed with 4% of paraformaldehyde, and snap frozen. Heart sections (5 μm) derived from either NTG (*A* and *B*), MyBP-C.wt (line 2/1) (*C* and *D*), or MyBP-C.mut1 (line 32) (*E* and *F*) animals were stained with the antibodies before viewing under confocal microscopy. (*A*) FC-18 detects endogenous MyBP-C in an NTG section. (*B*) Anti–C-Myc staining of NTG section. (*C*) Anti–C-Myc staining of TG MyBP-C.wt section shows the characteristic doublet, restricted to the A-band and is comparable to the staining in *A*. (*D*) A section derived from an MyBP-C.wt animal (line 2/1, 15 wk) was double stained with anti–C-Myc monoclonal antibody (red) and anti-desmin polyclonal antibody (green). The antibodies reveal the well-organized and discrete striation patterns in the MyBP-C.wt heart. (*E*) A section derived from an MyBP-C.mut1 animal was doubly stained with anti–C-Myc (in red) and anti–α-actinin (in green). The MyBP-C.mut1 (line 32, 14 wk) heart section shows a patchy striation pattern and is diffuse relative to the patterns observed in *A* and *C*. The α-actinin staining confirmed that the sarcomere in this particular section

in the normal staining pattern across the A-band. Confirming this aberrant incorporation/binding, the truncated MyBP-C, in contrast to the wild-type protein, did not copurify with the sarcomeric proteins when typical myofilament protein preparations were made, indicating that the mutated protein's association with the other contractile proteins was not robust enough to survive the biochemical extraction procedure (data not shown).

MyBP-C.mut1 mice exhibit histopathological and ultra-structural cardiac alterations. In the above confocal analyses, incorporation of the truncated protein was obviously abnormal. Therefore, we were interested in understanding the structural consequences of the mutant protein's incorporation as well as the presence of decreased amounts of normal MyBP-C upon the cardiomyocytes and sarcomeric structures in the affected hearts in mature animals. Gross examination of adults (25 wk) revealed no statistically significant cardiac hypertrophy and/or dilation in either the MyBP-C.wt line 2/1 or MyBP-C.mut1 (line 32) (Fig. 4) and no obvious hypertrophy has reproducibly presented in animals as old as 7 mo (data not shown). To date, no increases in morbidity or mortality are apparent within the colonies and, as is the case of the human population carrying the mutation (15, 30), upon superficial examination, all lines of the mice appear to be normal. However, histological sections prepared from the MyBP-C.mut1 hearts (line 32) revealed striking structural abnormalities, with numerous oval-shaped foci that stained with trichrome blue present within individual myocytes, as well as somewhat stronger blue staining in the interstitium (Fig. 4). This presented in each tissue layer in all four chambers of the hearts but was more frequent in the atria. MyBP-C.wt (line 2/1) as well as NTG hearts showed only the normal pattern of discrete blue staining in restricted interstitial areas.

Transmission electron microscopy was used to examine the ultrastructure of TG and NTG hearts using sections also derived from 25-wk-old animals. The NTG mice showed well-organized sarcomeres, with regularly aligned Z-bands, clear M-lines, and regularly distributed mitochondria, sarcoplasmic reticulum, and T-tubules (Fig. 5 *A*). In contrast, scattered degenerating myocytes, adjacent to overtly normal appearing cells, were found throughout all of the chambers of the MyBP-C.mut1 TG lines (Fig. 5 *B*). In ventricular myocytes in the early degenerative stages, only small areas adjacent to the nucleus showed a lack of sarcomeric organization; these areas contained scattered profiles of sarcoplasmic reticulum and a few mitochondria (Fig. 5 *C*). The remaining part of the cell appeared overtly normal although upon close examination of the myofibrils, subtle signs of disorganization could be detected with the T-tubules being slightly distended and some of the mitochondria exhibiting abnormal morphology. In the ventricular myocytes in the late stages of dysgenesis, the degenerated part of the cell contained some profiles of sarcoplasmic reticulum, lipid droplets, and a rim of myofibrils along the sarco-

retains its characteristic structure. (*F*) A section derived from an MyBP-C.mut1 line 32 cardiomyocyte in the late stages of dysgenesis was double stained with anti–C-Myc monoclonal antibody (red) and antidesmin polyclonal antibody (green). Unlike *D*, the staining patterns of the two proteins are not discrete and there is obvious disruption of the normal striated pattern. Scale bars: *A–F*, 100 μm.
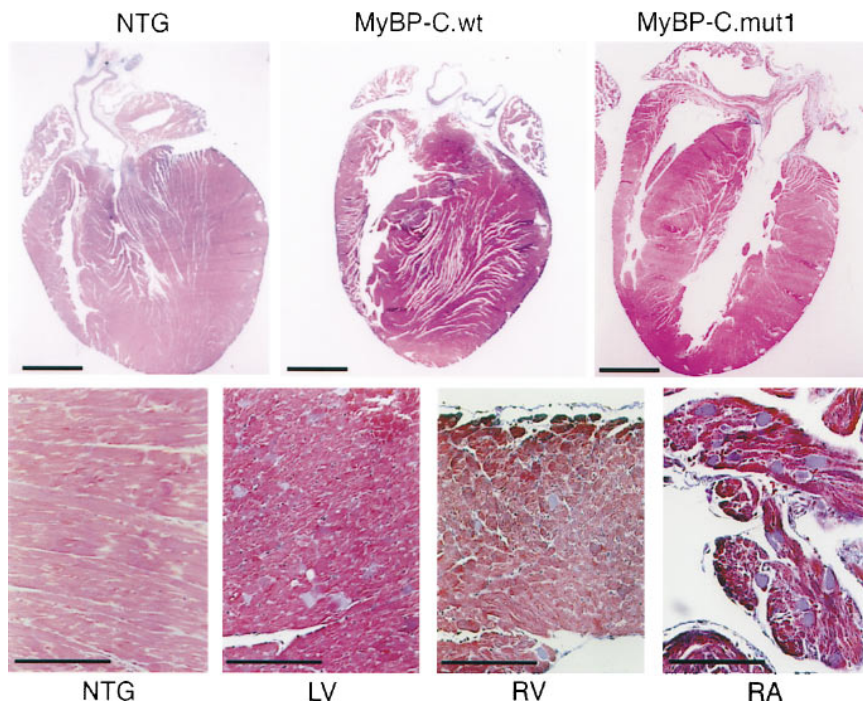
Figure 4. Histology of TG mouse hearts. (*Top*) Longitudinal sections of whole hearts stained with trichrome. (*Bottom*) Higher magnification views of trichrome-stained sections from the MyBP-C.mut1 ventricle and atria. Line 2/1 (MyBP-C.wt) and line 32 (MyBP-C.mut1) at 25 wk were used. Scale bars: *top*, 1 mm; and *bottom*, 1 mm.

lemma (Fig. 5, *B* and *E*). No collagen deposition was apparent in any part of the cell and histochemical staining for polysaccharides and glycogen was negative. Sections derived from the MyBP-C.wt hearts did not show the degenerative pattern.

Isolated ventricular fibers from MyBP-C.mut1 mice show increased Ca²⁺ sensitivity and decreased maximum relative power. In an attempt to detect functional changes, cardiac functions using both Langendorff and working heart preparations were carried out on mature adults (25 wk) from both the MyBP-C.wt and MyBP-C.mut1 lines. No differences in contraction, relaxation, or in the hearts' responses to increased workload could be discerned (data not shown). Subsequently, mechanical analyses of skinned fiber strips from the left ventricular papillary muscles of the TG mice and their NTG littermates were performed. These analyses were normally carried out on the youngest mice possible (3–4 wk) that showed steady-state levels of TG protein, in order that any changes detected in the fiber kinetics were a result of the primary isoform change, not secondary compensatory processes that might be occurring. Preliminary experiments in which the wild-type overexpresser line 2/1 fibers were compared with those derived from NTG littermates revealed no detectable differences. Even when fibers were compared from older mice (8–10 wk), there were no differences (Fig. 6 *A*), indicating that incorporation of the wild-type protein has no effect on the fiber's sensitivity to Ca²⁺.

In contrast to these results, the MyBP-C.mut1 fibers showed significant changes in both power output and Ca²⁺ sensitivity to force development. A leftward shift in the pCa–force relationship was apparent (Fig. 6 *B*) and the maximum relative power (Fig. 6 *D*), derived from the intermediate portion of the force–power curve, was significantly decreased (Fig. 6, *C* and *D*). No differences between the MyBP-C.wt fibers and those derived from their NTG littermates could be detected and there were no differences among all groups in other

parameters, such as unloaded shortening velocity and maximum shortening velocity (data not shown).

Discussion

This study uses a TG paradigm to remodel an abundant protein specifically in the cardiac compartment. As shown previously for the myosin light chains (25, 29), the cardiomyocyte is apparently able to regulate the overall stoichiometry of MyBP-C such that significant TG overexpression does not change overall stoichiometry of the protein's pool. Rather, a partial replacement dependent upon the degree of overexpression occurs. Analyses of TG mice overexpressing the normal isoform ensured that merely overexpressing MyBP-C did not result in a detectable phenotype, while the addition of a C-Myc epitope at the NH₂ termini allowed us to distinguish and localize the TG proteins. Previous in vitro studies showed that the C-Myc epitope tag at this location does not interfere either with normal sarcomerogenesis or the recombinant MyBP-C's capability to incorporate into the sarcomere (17) and our results are consistent with these data.

Despite the well-established genetic etiologies (31, 32), the pathogenic processes leading to FHC remain obscure. Longitudinal pathological changes linked to the disease state in these patients are hard to obtain because of the nature of the disease. This has been particularly true for the MyBP-C related FHCs which consist, for the most part, of mutations that cause truncations of the COOH terminus containing the myosin binding site and, in some cases, the titin binding site as well. Mutations in this protein account for a significant percentage of genetically defined FHC cases (15–20%), but the symptoms are quite mild with diagnosis depending upon noninvasive echocardiographic procedures (15, 21, 30). Since FHC is an autosomal dominant disease (patients are heterozygous), the TG approach of expressing a mutant protein in an attempt to
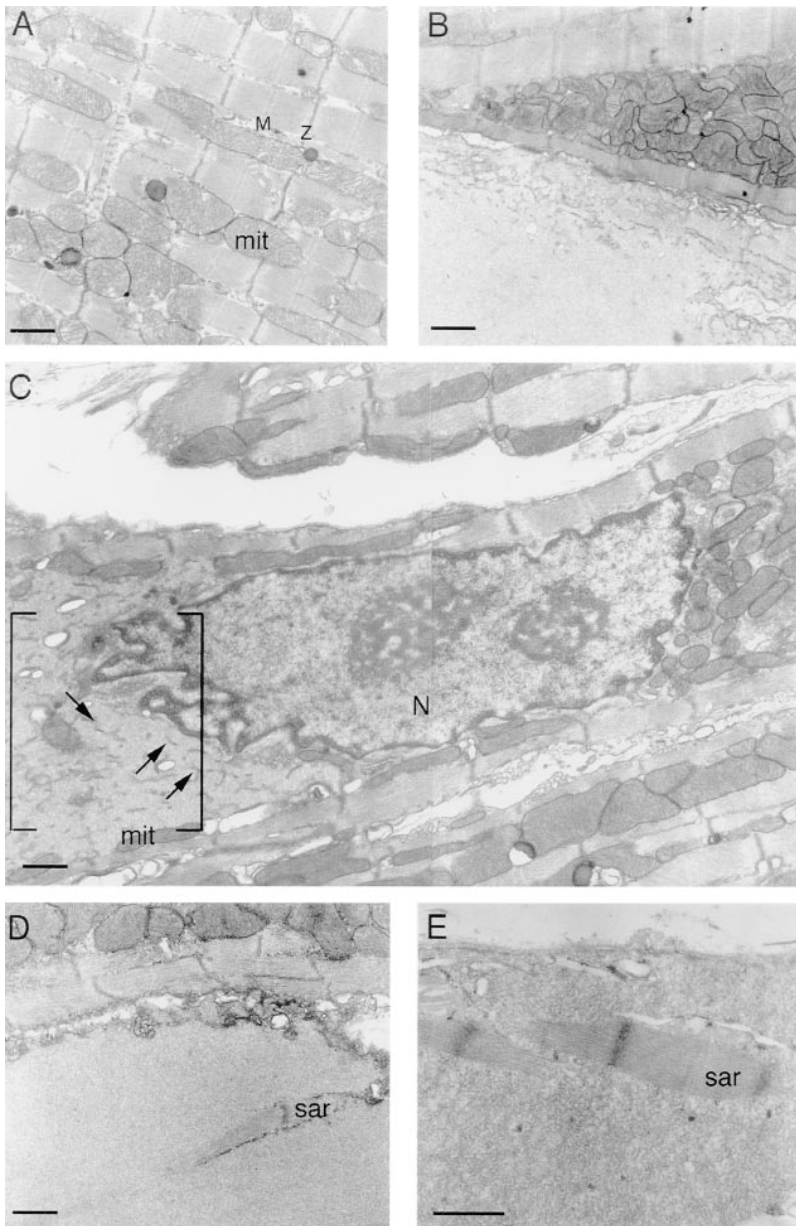
Figure 5. Electron microscopy of left ventricular myocardium from MyBP-C.wt mice. (*A*) The NTG control sections all showed well-organized sarcomeres, with regularly aligned Z-bands (*Z*), clear M-lines (*M*), and regularly distributed mitochondria (*mit*), sarcoplasmic reticulum, and T-tubules. (*B*) Scattered degenerating myocytes were found throughout all of the chambers of the MyBP-C.mut1 TG lines. Shown is typical morphology presented by an affected cardiomyocyte (*bottom*), adjacent to an overtly normal (*top*) appearing cell. (*C*) Example of a ventricular myocyte in the early degenerative stage. Small areas (*bracket*) adjacent to the nucleus (*N*) showed a lack of sarcomeric organization; this area contained scattered profiles of sarcoplasmic reticulum (*arrows*) and a few mitochondria (*mit*). The remaining part of the cell appeared grossly normal although, upon close examination of the myofibrils, subtle signs of disorganization could be detected, with the T-tubules being slightly distended and some of the mitochondria exhibiting abnormal morphology. (*D* and *E*) Examples of ventricular myocytes in the late degenerative stages. Cell cytoplasm contains some profiles of sarcoplasmic reticulum, lipid droplets, and a rim of myofibrils along the sarcolemma. Single, partial isolated sarcomeres (*sar*) can be detected. No collagen deposition was apparent in any part of the cell and histochemical staining for polysaccharides and glycogen was negative. MyBP-C.mut1 sections were derived from 25-wk, line 2/1 left ventricles. Sections derived from the MyBP-C.wt hearts did not show cardiomyocyte degeneration. Scale bars: *A–E*, 1 μm.

model the disease is feasible, provided that overall protein stoichiometry is not perturbed by changes in gene dosage. For MyBP-C, this appears to be the case.

A recent case study used endomyocardial biopsies to obtain information concerning the RNA and protein levels in an MyBP-C–linked FHC patient. The subject contained an MyBP-C gene in which premature termination of the transcript presumably led to the production of a protein lacking the myosin binding site and at least part of the titin binding site; it terminates within the C9 domain (Fig. 1 *A*). Although a shortened transcript was present, Western analysis could not detect the truncated protein, leading the authors to conclude that it was unstable or that other, undefined mechanisms came into play (21). This does not appear to be the case for the particular mutation in our model, as we can easily detect intact truncated protein using either Western analysis or by standard staining on SDS-PAGE. However, it should be emphasized that steady-state levels of a mutant protein are probably mutation-

specific and the human biopsies did contain a different MyBP-C mutation than is represented by MyBP-C.mut1 (Fig. 1 *A*).

The mutated protein is incorporated into the sarcomere, albeit in an aberrant fashion. While the TG wild-type MyBP-C is efficiently and correctly incorporated into the A-bands of the myofilaments in the MyBP-C.wt TG mice in a manner indistinguishable from the endogenous protein, the truncated MyBP-C does not display a normal striated pattern. Immunostaining with anti–C-Myc shows an abnormal striation pattern and/or diffuse staining. Costaining of these sections with anti–MyBP-C and antidesmin/α-actinin antibodies demonstrated that MyBP-C. mut1 protein was no longer restricted to the (normal) A-band location but was present, presumably in the I-band and Z-bands, as well as being diffused in the cytoplasm. These data, along with the inability of the truncated protein to copurify with the other contractile proteins using standard myofilament preparations, demonstrate that cardiac MyBP-C protein lacking titin and myosin binding domains,
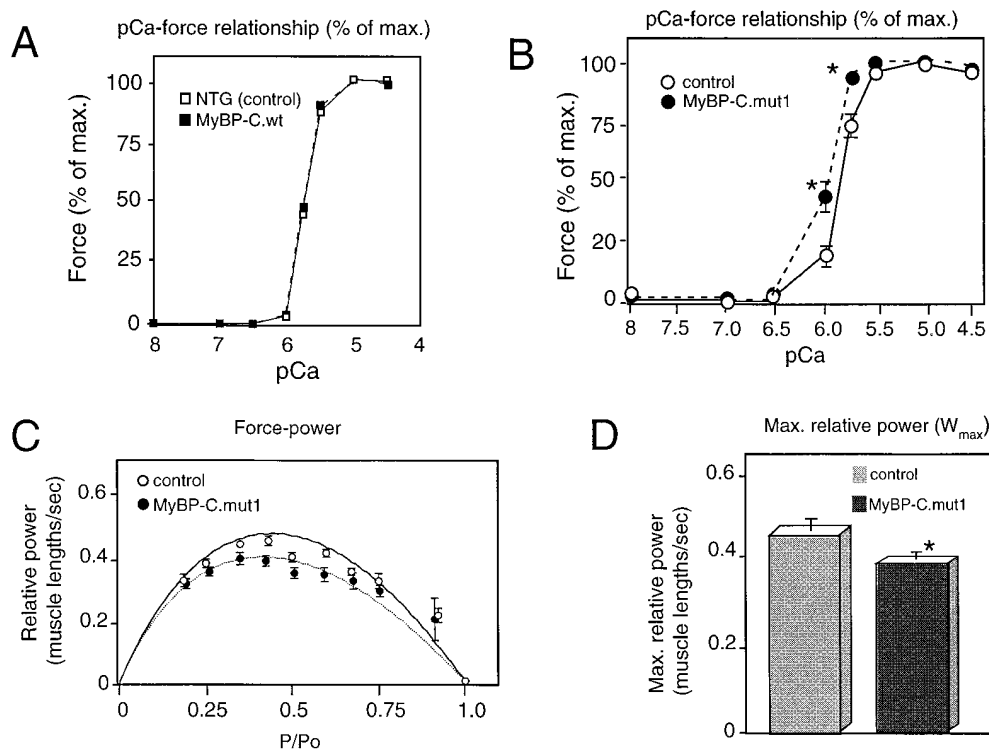
Figure 6. Contractile properties of permeabilized ventricular fibers. Mechanical analysis of skinned fiber strips from left ventricular papillary muscles of MyBP-C.wt (line 2/1, 8–10 wk), MyBP-C.mut1 TG mice (line 32, 3–4 wk), and their NTG littermates (control). (*A*) The pCa–force relationship. Force generated from mouse left ventricular papillary muscles as a function of $[Ca^{2+}]$. Force is expressed as percent force achieved at maximal Ca^{2+} activation. The free Ca^{2+} concentration is expressed as $-\log Ca^{2+}$ (*pCa*). Incorporation of the wild-type protein (line 2/1) had no effect on the pCa–force relationship. (*B*) Note the significant left shift of the curve for the TG fibers derived from MyBP-C.mut1. (*C*) Relative power plots. (*D*) Maximum relative power. Significant differences present in the maximum relative power output between the MyBP-C.mut1 and NTG fibers. $*P < 0.05$.

while present in the sarcomere, is not incorporated correctly and is only weakly associated with the contractile apparatus.

These results are in striking contrast to those obtained with other FHC models studied to date. In both a gene knockout (33) and TG (34) model of FHC caused by mutation(s) in the MyHC, an obvious dominant-negative effect presented. Clearly, a pronounced dominant-negative effect at the whole animal level is lacking or severely attenuated for the particular mutation with which we are dealing. This also appears to be the case in the human population with this mutation (30). Our analyses suggest that haploinsufficiency, in which the disease progresses very slowly due to decreased levels of endogenous protein (the "null allele" hypothesis), could play a major role in the pathogenic process, at least for the set of mutations which lack completely both the myosin and titin binding sites. However, it should be emphasized that this may not hold for other classes of MyBP-C mutations and one could envision more strongly dominant-negative mutations in which a (different) truncated MyBP-C could indeed be a more active "poison peptide."

The histopathological and ultrastructural abnormalities in the MyBP-C.mut1 mice illustrate the structural consequences caused by the lack of enough functioning MyBP-C incorporation in the sarcomeric assembly and/or incorporation of the aberrant polypeptide. In heart sections stained with trichrome, blue staining cells were scattered throughout all of the cardiac chambers, but the density was increased in the atria, presumably because of the transgene's expression in this compartment early in development (35). We noted that the pathology was dose-related, with the frequency of dropout significantly reduced in the lower expressing lines in which the endogenous protein is not replaced to the same degree as in the higher expressing lines.

Despite these structural changes, the phenotype of these mice is surprisingly mild during development and early adulthood, mirroring the relatively benign clinical picture of the MyBP-C–linked FHCs. While analyses at the whole organ level were uninformative, at the skinned fiber level, using very young animals in which cardiomyocyte degeneration had not yet presented, significant changes in the maximum relative power and the sensitivity of force production to Ca^{2+} levels could be discerned, indicating that subtle alterations in force production occur. Although there is no apparent heart enlargement and myocardium wall thickening in the MyBP-C. mut1 hearts, to date we have not yet obtained a large, aged cohort of animals suitable for detailed morphometric and stress exercise analyses (36). Previously, in other mouse models we have detected very early signs of hypertrophy using RNA analyses (37). However, molecular markers of hypertrophy such as β-MyHC, α-skeletal actin, and atrial natriuretic factor were not present in RNA derived from 6-mo MyBP-C.mut1 line 32 animals (data not shown). We suspect that the hypertrophic process in these mice is very slow or minimal, despite the scattering of dysfunctional cells in the myocardium. Consistent with this hypothesis, immunostaining and ultrastructural analyses of a very limited number of older (> 30 wk) animals showed a high degree of myocyte disarray and the nuclei, as visualized by electron microscopy, displayed the highly convoluted periphery characteristic of cardiomyocytes undergoing hypertrophy (data not shown). These data are particularly intriguing in light of clinical data that show onset of MyBP-C–FHC occurs much later in life than the FHCs caused by mutations in other contractile proteins (38). Again, it will be necessary to study a large, aged cohort of animals in order to define these processes completely.

It seems likely that both the null allele and poison peptide considerations are relevant to the phenotype and their relative importance may vary considerably depending upon the particular MyBP-C mutation. For example, as noted above, a more pronounced dominant-negative phenotype may present if an

MyBP-C lacking only the myosin binding site but containing most of the titin binding site is expressed, as this protein might insert more efficiently, yet still incorrectly into the sarcomere. The data clearly show that transgenesis will be useful in testing this and related hypotheses, as well as determining the basic structure–function relationships in both the normal and mutated forms of MyBP-C. The ability to generate multiple lines of mice exhibiting various degrees of TG expression will allow dose–response curves to be generated in which the time of onset, severity, and progression of the disease can be correlated with varying levels of the mutated protein. This should enhance the general usefulness of this group of animals as a model for studying in detail the longitudinal pathological processes involved in the disease's onset and progression late in life. These studies are ongoing.

Acknowledgments

References

1. Maron, B.J. 1996. Triggers for sudden cardiac death in the athlete. *Card. Clinics.* 14:195–210.

2. Geisterfer-Lowrance, A.A., S. Kass, G. Tanigawa, H.P. Vosberg, W. McKenna, C.E. Seidman, and J.G. Seidman. 1990. A molecular basis for familial hypertrophic cardiomyopathy: a beta cardiac myosin heavy chain gene missense mutation. *Cell.* 62:999–1006.

3. Bonne, G., L. Carrier, J. Bercovici, C. Cruaud, P. Richard, B. Hainque, M. Gautel, S. Labeit, M. James, J. Beckmann, et al. 1995. Cardiac myosin binding protein-C gene splice acceptor site mutation is associated with familial hypertrophic cardiomyopathy. *Nat. Genet.* 11:438–440.

4. Kimura, A., H. Harada, J.-E. Park, H. Nishi, M. Satoh, M. Takahashi, S. Hiroi, T. Sasaoka, N. Ohbuchi, T. Nakamura, et al. 1997. Mutations in the cardiac troponin I gene associated with hypertrophic cardiomyopathy. *Nat. Genet.* 16:379–382.

5. Poetter, K., H. Jiang, S. Hassanzadeh, S.R. Master, A. Chang, M.C. Dalakas, I. Rayment, J.R. Sellers, L. Fananapazir, and N.D. Epstein. 1996. Mutations in either the essential or regulatory light chains of myosin are associated with a rare myopathy in human heart and skeletal muscle. *Nat. Genet.* 13:63–69.

6. Thierfelder, L., H. Watkins, C. MacRae, R. Lamas, W. McKenna, H.P. Vosberg, J.G. Seidman, and C.E. Seidman. 1994. Alpha-tropomyosin and cardiac troponin T mutations cause familial hypertrophic cardiomyopathy: a disease of the sarcomere. *Cell.* 77:701–712.

7. Watkins, H., W.J. McKenna, L. Thierfelder, H.J. Suk, R. Anan, A. O'Donoghue, P. Spirito, A. Matsumori, C.S. Moravec, J.G. Seidman, and C.E. Seidman. 1995. Mutations in the genes for cardiac troponin T and alpha-tropomyosin in hypertrophic cardiomyopathy. *N. Engl. J. Med.* 332:1058–1064.

8. MacRae, C.A., N. Ghaisas, S. Kass, S. Donnelly, C.T. Basson, H.C. Watkins, R. Anan, L.H. Thierfelder, K. McGarry, and E.E.A. Rowland. 1995. Familial hypertrophic cardiomyopathy with Wolff-Parkinson-White syndrome maps to a locus on chromosome 7q3. *J. Clin. Invest.* 96:1216–1220.

9. Trinick, J. 1996. Titin as a scaffold and spring. Cytoskeleton. *Curr. Biol.* 6:258–260.

10. Offer, G., C. Moos, and R. Starr. 1973. A new protein of the thick filaments of vertebrate skeletal myofibrils. Extraction, purification and characterization. *J. Mol. Biol.* 74:653–676.

11. Freiburg, A., and M. Gautel. 1996. A molecular map of the interactions between titin and myosin-binding protein C. Implications for sarcomeric assembly in familial hypertrophic cardiomyopathy. *Eur. J. Biochem.* 235:317–323.

12. Seiler, S.H., D.A. Fischman, and L.A. Leinwand. 1996. Modulation of myosin filament organization by c-protein family members. *Mol. Biol. Cell.* 7:113–127.

13. Watkins, H., D. Conner, L. Thierfelder, J.A. Jarcho, C. MacRae, W.J. McKenna, B.J. Maron, J.G. Seidman, and C.E. Seidman. 1995. Mutations in the cardiac myosin binding protein-C gene on chromosome 11 cause familial hypertrophic cardiomyopathy. *Nat. Genet.* 11:434–437.

14. Yu, B., J.A. French, L. Carrier, R.W. Jeremy, D.R. McTaggart, M.R. Nicholson, B. Hambly, C. Semsarian, D.R. Richmond, K. Schwartz, and R.J. Trent. 1998. Molecular pathology of familial hypertrophic cardiomyopathy caused by mutations in the cardiac myosin binding protein C gene. *J. Med. Genet.* 35:205–210.

15. Moolman-Smook, J.C., B. Mayosi, P. Brink, and V.A. Corfield. 1998. Identification of a new missense mutation in MyBP-C associated with hypertrophic cardiomyopathy. *J. Med. Genet.* 35:253–254.

16. Carrier, L., G. Bonne, E. Bahrend, B. Yu, P. Richard, F. Niel, B. Hainque, C. Cruaud, F. Gary, S. Labeit, et al. 1997. Organization and sequence of human cardiac myosin binding protein C gene (MYBPC3) and identification of mutations predicted to produce truncated proteins in familial hypertrophic cardiomyopathy. *Circ. Res.* 80:427–434.

17. Gilbert, R., M.G. Kelly, T. Mikawa, and D.A. Fischman. 1996. The carboxyl terminus of myosin binding protein C (MyBP-C, C-protein) specifies incorporation into the A-band of striated muscle. *J. Cell Sci.* 109:101–111.

18. Okagaki, T., F.E. Weber, D.A. Fischman, K.T. Vaughan, T. Mikawa, and F.C. Reinach. 1993. The major myosin-binding domain of skeletal muscle MyBP-C (C protein) resides in the COOH-terminal, immunoglobulin C2 motif. *J. Cell Biol.* 123:619–626.

19. Sweitzer, N.K., and R.L. Moss. 1993. Determinants of loaded shortening velocity in single cardiac myocytes permeabilized with alpha-hemolysin. *Circ. Res.* 73:1150–1162.

20. Schwartz, K. 1995. Familial hypertrophic cardiomyopathy. Nonsense versus missense mutations. *Circulation.* 91:2865–2867.

21. Rottbauer, W., M. Gautel, J. Zehelein, S. Labeit, W.M. Franz, C. Fischer, B. Vollrath, G. Mall, R. Dietz, W. Kübler, and H.A. Katus. 1997. Novel splice donor site mutation in the cardiac myosin-binding protein-C gene in familial hypertrophic cardiomyopathy. *J. Clin. Invest.* 100:475–482.

22. Kasahara, H., M. Itoh, T. Sugiyama, N. Kido, H. Hayashi, H. Saito, S. Tsukita, and N. Kato. 1994. Autoimmune myocarditis induced in mice by cardiac C-protein. Cloning of complementary DNA encoding murine cardiac C-protein and partial characterization of the antigenic peptides. *J. Clin. Invest.* 94:1026–1036.

23. Palermo, J., J. Gulick, M. Colbert, J. Fewell, and J. Robbins. 1996. Transgenic remodeling of the contractile apparatus in the mammalian heart. *Circ. Res.* 78:504–509.

24. McAuliffe, J.J., and J. Robbins. 1991. Troponin T expression in normal and pressure-loaded fetal sheep heart. *Pediatr. Res.* 29:580–585.

25. Fewell, J., T.E. Hewett, R. Klevitsky, E. Hayes, D. Warshaw, A. Sanbe, D. Maughan, and J. Robbins. 1998. Functional significance of cardiac myosin essential light chain isoform switching in transgenic mice. *J. Clin. Invest.* 101:2639–2651.

26. Edman, K.A.P. 1979. The velocity of unloaded shortening and its relation to sarcomere length and isometric force in vertebrate muscle fibers. *J. Physiol.* 291:143–159.

27. Moss, R. 1986. Effects on shortening velocity of rabbit skeletal muscle due to variations in the level of thin-filament activation. *J. Physiol.* 377:487–505.

28. Muthuchamy, M., P. Rethinasamy, and D.F. Wieczorek. 1997. Tropomyosin structure and function. *Trends Cardiovasc. Med.* 7:124–128.

29. Gulick, J., T.E. Hewett, R. Klevitsky, S. Buck, R.L. Moss, and J. Robbins. 1997. Transgenic remodeling of the regulatory myosin light chains in the mammalian heart. *Circ. Res.* 80:655–664.

30. Charron, P., O. Dubourg, M. Desnos, R. Isnard, A. Hagege, G. Bonne, L. Carrier, F. Tesson, J.B. Bouhour, J.C. Buzzi, et al. 1998. Genotype-phenotype correlations in familial hypertrophic cardiomyopathy. A comparison between mutations in the cardiac protein-C and the beta-myosin heavy chain genes. *Eur. Heart J.* 19:139–145.

31. Seidman, C.E., and J.G. Seidman. 1998. Gene defects that cause inherited cardiomyopathy. *In* The Molecular Basis of Heart Disease. W.B. Saunders Co., Philadelphia, PA.

32. Watkins, H. 1994. Multiple disease genes cause hypertrophic cardiomyopathy. *Br. Heart J.* 7296(Suppl.):S4–S9.

33. Geisterfer-Lowrance, A.A., M. Christe, D.A. Conner, J.S. Ingwall, F.J. Schoen, C.E. Seidman, and J.G. Seidman. 1996. A mouse model of familial hypertrophic cardiomyopathy. *Science.* 272:731–734.

34. Vikstrom, K.L., S.M. Factor, and L.A. Leinwand. 1996. Mice expressing mutant myosin heavy chains are a model for familial hypertrophic cardiomyopathy. *Mol. Med.* 2:556–567.

35. Ng, W.A., I.L. Grupp, A. Subramaniam, and J. Robbins. 1991. Cardiac myosin heavy chain mRNA expression and myocardial function in the mouse heart. *Circ. Res.* 68:1742–1750.

36. Fewell, J.G., H. Osinska, R. Klevitsky, W.E. Ng, G. Sfyris, F. Bahrehmand, and J. Robbins. 1997. A treadmill exercise regimen for identifying subtle cardiovascular phenotypes in transgenic mice. *Am. J. Physiol.* 273:H1595–H1605.

37. Jones, W.K., I.L. Grupp, T. Doetschman, G. Grupp, H. Osinska, T.E. Hewett, G. Boivin, J. Gulick, W.A. Ng, and J. Robbins. 1996. Ablation of the murine alpha myosin heavy chain gene leads to dosage effects and functional deficits in the heart. *J. Clin. Invest.* 98:1906–1917.

38. Niimura, H., L.L. Bachinski, S. Sangwatanaroj, H. Watkins, A.E. Chudley, W. McKenma, A. Kristinsson, R. Roberts, M. Sole, B.J. Maron, et al. 1998. Mutations in the gene for cardiac myosin-binding protein C and late-onset familial hypertrophic cardiomyopathy. *N. Engl. J. Med.* 338:1248–1257.